J Mater Sci: Mater Med (2009) 20:1115–1129
DOI 10.1007/s10856-008-3655-3

TecoflexTM functionalization by curdlan and its effect on protein adsorption and bacterial and tissue cell adhesion

Anand P. Khandwekar · Deepak P. Patil · Vaibhav Khandwekar · Yogesh S. Shouche · Shilpa Sawant · Mukesh Doble

Received: 1 August 2008 / Accepted: 24 November 2008 / Published online: 18 December 2008

Abstract Curdlan modified polyurethane was created by physically entrapping the former on TecoflexTM surface. ATR-FT-IR, SEM-EDAX and AFM analysis revealed the formation of stable thin curdlan layer on the film. Contact-angle measurements showed that the modified film was highly hydrophilic. Confocal laser scanning microscopy showed the existence of entrapped layer of approximately 20–25 μm in depth. Surface entrapment of curdlan minimized both protein adsorption and mouse L929 fibroblast cell adhesion relative to the control. Surface induced cellular inflammatory response was determined from the expression levels of proinflammatory cytokine TNF-α, by measuring their mRNA profiles in the cells using real time polymerase chain reaction (RT-PCR) normalized to the housekeeping gene GAPDH. The inflammatory response was suppressed on the modified substrate as expression of TNF-α mRNA was found to be up regulated on TecoflexTM, while it was significantly lower on curdlan substrate. The adhesion of *S. aureus* decreased by 62% on curdlan modified surface. Using such simple surface entrapment process, it will be possible to develop well-defined surface modifications that promote specific cell interactions and perhaps better performance in the long-term as implant.

A. P. Khandwekar · M. Doble (✉)
Department of Biotechnology, Indian Institute of Technology Madras, Chennai 600036, India
e-mail: mukeshd@iitm.ac.in

D. P. Patil · Y. S. Shouche
National Center for Cell Science, Ganeshkhind, Pune 411007, India

V. Khandwekar
Visvesvaraya National Institute of Technology, Nagpur 440011, India

S. Sawant
Bhabha Atomic Research Center, Trombay, Mumbai 400085, India

1 Introduction

In recent years, researchers have focused on the development of bioinert and biocompatible coatings which can be used to minimize non-specific adhesion and inflammatory events but at the same time maintain the physicochemical properties of the material. The attachment of proteins and cells to materials is biologically significant as it can cause postoperative complications in medical implants, subsequently leading to failure. It is well recognized that protein adsorption on neutral hydrophilic surfaces tends to be relatively weak and therefore, to increase their hydrophilicity, hydrogels or polymer brushes have been widely used to modify biomaterial surfaces. Such modified surfaces, which exhibit minimal cell-adhesion, are believed to mimic the natural non-adhesive characteristics of the endothelial cell glycocalyx. The endothelial glycocalyx, a hydrated structure rich in proteoglycans, glycosaminoglycans, and proteins plays a significant role in maintaining the normal non-adhesive and biocompatible properties of the native intravascular luminal wall [1–4]. A significant challenge in engineering a biomimetic surface on biomaterials is to achieve a high surface density of biomolecules. Typical biomaterials are hydrophobic, with no labile chemical

groups that might be used with conventional immobilization strategies [5]. The current limitation in utilizing biomolecules as surface coatings is that some of the reagents used for surface coupling are highly toxic, expensive, and require stringent anhydrous reaction conditions [6, 7]. The unique mechanical and biological properties make polyurethanes (PUs) as ideal materials for many implantable devices. However, uncertain long-term biostability in the human physiological environment limits their extensive clinical applications. Chronic inflammatory response associated with cellular activation has been suggested as one of the prime factors for their failure, although the mechanism of this response to the surfaces is still unknown [8]. Medical grade TecoflexTM has been chosen as a model substrate in this study since it has extensive applications in a variety of biomedical devices [9, 10].

Curdlan is a member of the family of bacterial polysaccharides approved as food additives by the USFDA [11–14]. It is a linear hydrophilic polysaccharide produced by *Alcaligenes faecalis* with no branching and because of its non-ionic gel-forming properties it is considered as a potentially important matrix for life science applications [11, 12]. Curdlan potentially has an inhibitory effect against AIDS virus infection and blood anti-coagulant activity, as well as low toxicity in vitro and in vivo [13–15]. In this work, TecoflexTM surface was engineered with curdlan by entrapping it during the reversible swelling of the polymer surface region. A critical design feature of this surface is to use the protruding curdlan oligosaccharides to mimic the non-adhesive properties of a glycocalyx. With such a protein and cell-resistant biomaterial surface as a foundation, the multivalent nature of curdlan could also be exploited for high density surface immobilization of extracellular matrix-based peptides for precisely controlling, specific cell interactions. Bovine serum albumin does not contain the peptide sequences necessary for cells to adhere and is often used to passivate blood contacting materials [16, 17]. Hence, in the present study the performance of the curdlan modified surface was compared with that of BSA modified surface.

The entrapment technique followed in the present work is based on the method reported by Desai and Hubbell, which does not involve any toxic reagents but uses only aqueous solutions and also follows mild reaction conditions. This method is also named as surface physical interpenetrating network (SPIN) [18–20]. Surface changes after the modification process was extensively probed with several spectroscopic and microscopic analytical tools. The in vitro biocompatibility of the modified polymers was ascertained by evaluating their resistance to protein adsorption, cell attachment, and bacterial adhesion. The cellular inflammatory response was investigated using real-time reverse transcription polymerase chain reaction (RT-PCR).

2 Materials and methods

2.1 Surface entrapment process

TecoflexTM (EG-93A-B40) was obtained in the form of granules as a gift from Devon Innovations, Bengaluru (India). A 50 mg/ml solution in tetrahydrofuran (Merck) was used to cast films of 1.5 mm wet thickness using a casting knife. These films were cured for 6 h in an oven at 60°C to evaporate the solvent. The surface modifying solution was then prepared by first dissolving curdlan (Sigma, M.W of 1×10^5 Da) in 0.25 M NaOH, and then adding tetrahydrofuran to it. The resultant mixture consisted of 20% w/v of curdlan and 45% v/v of THF and 40% v/v of deionized filtered water (DIFW). In the case of bovine serum albumin (Himedia, M.W. 66,000 Da), it was dissolved in a miscible mixture of water–acetone (70:30 v/v), followed by the addition of THF to arrive at a solution of 20% w/v of BSA and 45% v/v of THF and 40% v/v of DIFW. Rhodamine-labeled dextran (Sigma, M.W 40,000 Da) was dissolved in a DIFW, followed by the addition of THF to arrive at a solution of 20% w/v of rhodamine-labeled dextran, 45% v/v of THF and 40% v/v of DIFW. TecoflexTM films were immersed in 10 ml of this solvent/nonsolvent mixture for 24 h, and were then quenched with an excess of nonsolvent ($\sim$20 ml DIFW). The films were removed from this solution, washed with water, and then dried overnight in a desiccator. Exposure of the polymer to THF in the absence of these molecules resulted in much faster polymer–solvent interaction, and therefore an estimation of the equivalent treatment time (as determined visually) that created the same degree of surface swelling was used as a control to account for possible residual solvent effects on the cell behaviour.

2.2 Physical adsorption

The TecoflexTM films were incubated with 20% w/v curdlan in 0.25 M NaOH or 20% w/v BSA in PBS, at 37°C for 24 h. Following the treatment the samples were gently washed once in PBS.

2.3 Surface characterization

The modified surfaces were extensively probed with various spectroscopic and microscopic techniques which are described below. Hereby, for convenience TecoflexTM, Curdlan modified TecoflexTM and BSA modified

TecoflexTM will be abbreviated as PU, PU-Curdlan and PU-BSA respectively.

2.3.1 *Attenuated total reflection-fourier transform infrared spectroscopy (ATR)-FT-IR*

ATR-FTIR spectra of the base and modified TecoflexTM samples were obtained using FT/IR-4200 (Jasco, Netherlands) spectrometer having a baseline horizontal ATR accessory. Films were pressed against Zn–Se crystal and the spectra were collected at a resolution of 4 cm^{-1}.

2.3.2 *Dynamic contact-angle measurements, surface free energy and in vitro stability of surface films*

The surface hydrophobicity and heterogeneity of the biomaterials were determined by measuring the advancing and receding contact angles (θ_A and θ_R; respectively) using a Krüss Easy drop goniometer (KRUSS, DSA II GmbH, Germany). Ultrapure water was used as the contact angle liquid, and mean values were determined by averaging the measurements on at least five independent specimens. The surface free energy of the samples were calculated using Fowkes's method, based on measurements using three probe liquids, namely Diiodomethane (Sigma), Formamide (Sigma) and water (Ultrapure).

The stability of the entrapped molecules on PU was assessed by placing the samples in 5 ml of 0.9% NaCl solution at 37°C for various time periods. After 5, 10, 20, and 30 days, the samples were retrieved and rinsed with copious amount of distilled water and their static contact angles were measured. The measurements were performed at three different spots on the surface and the average readings were reported.

2.3.3 *Scanning electron microscopy and energy dispersive X-ray analysis (SEM-EDAX)*

Energy dispersive X-ray analysis was performed to identify and quantify the elemental composition on the surfaces with the help of a Jeol Scanning electron microscope (Model JSM 6380, Japan). The surfaces were coated with a thin layer of platinum and the micrographs were taken at a secondary electron imaging mode. The excitation energy for these measurements was 15 keV, with analysis time of 100 s. The ZAF program, which does not require the presence of any internal standard, was used to calculate the elemental composition of the surface [21, 22].

2.3.4 *Atomic force microscopy (AFM)*

AFM studies were performed using a scanning probe microscope (SPM-Solver P47, NT-MDT, Russia) in contact mode. Rectangular cantilever of silicon nitride (length 200 μm and width 40 μm) having a force constant of 3 N/m was employed for the measurement. The various roughness parameters were obtained using the software provided with the AFM. Maximum roughness (R_{max}) is the difference between the maximum and minimum values of z coordinate on the surface within the analysis area. R_{mean} is calculated using the following formula:

$$R_{mean} \equiv Z_{mean} = \frac{1}{N_x N_y} \sum_{i=1}^{N_x} \sum_{j=1}^{N_y} Z_{ij}$$

where, Z_{ij} is the z-coordinate value, and the average roughness is given by the (R_a) following formula:

$$R_a = \frac{1}{N_x N_y} \sum_{i=1}^{N_x} \sum_{j=1}^{N_y} |z(i,j) - Z_{mean}|$$

N_x and N_y are the number of measurements in the x and y direction.

2.3.5 *Confocal laser scanning microscopy (CLSM)*

To characterize the entrapment of the biomacromolecules on the surface of the TecoflexTM film, rhodamine-labeled dextran was immobilized on it following the same procedure and it was investigated using a confocal laser scanning microscopy (Nikon A1 confocal laser scanning microscope). The laser wavelength of 543 nm was applied to excite the dye and images were collected as a stack of 2-dimensional optical sections by digitizing sequential series of images while focusing down through the specimen using a computer-controlled stepping motor.

2.4 Protein adsorption

Bovine fibrinogen (Himedia, India) in the form of a lyophilized powder was dissolved in PBS and maintained at a pH of 7.4. The amount of adsorbed protein on the polymer surfaces was estimated using 125I-labelled protein. This protein was added to unlabelled protein solution to obtain a final activity of approximately 10^7 cpm/mg. The polymer samples were immersed in 1 ml buffer solution at 37°C, and then 1 ml fibrinogen solution (0.2 mg/ml) was added and mixed. After 1 h, samples were rinsed three times with 2 ml of PBS. The gamma activities were counted with the samples placed in radio-immunoassay tubes by a Gamma counter (Perkin Elmer, USA). Three parallel replicates were used. The counts from each sample were averaged and the surface concentration was calculated from the following equation

$$\mathrm{BFG}\,(\mu g/cm^2) = \mathrm{Counts}\,(\mathrm{cpm})\; C_{\mathrm{solution}}(\mu g/ml)/ [A_{\mathrm{solution}}(\mathrm{cpm/ml}) \times S_{\mathrm{sample}}(cm^2)]$$

where the count is the radioactivity of the samples, the S_{sample} is the surface area of the samples, C_{solution} and A_{solution} are the concentration and the specific activity of the protein solution, respectively.

2.5 Short-term bacterial adhesion assays

The two key organisms that are associated with implant related infections are gram-positive *Staphylococcus aureus* (NCIM 5021) and gram-negative *Pseudomonas aeruginosa* (NCIM 5029), so adhesion of these two bacterial species was assessed. Hundred millilitres of nutrient broth (Himedia, India) was inoculated with a single colony of bacteria from a tryptone soya agar (Himedia, India) stock plate. The broth was incubated at 37°C overnight in a shaking incubator and was split between 2 falcon tubes and centrifuged at 3,500 rpm for 20 min. Cells were resuspended in phosphate buffered saline. This was repeated twice more and the cells were finally resuspended at a concentration of 1×10^8 cells/ml. Three discs of each polymer were placed in a 24 well plate and were incubated in 1 ml of the cell suspension for 4 h at 37°C in a shaking incubator and rinsed twice with PBS. The bacterial cells were eluted from the surfaces into 2 ml sterile PBS using an ultrasonic cleaner (Cole-Parmer, 8891EDTH, USA). The procedure involved 4 min sonication followed by 1 min mild vortexing (repeated three times). A known volume of the sample was inoculated into Tryptone Soya agar and incubated at 37°C for 24 h. The colony forming units were counted, which was an indication of the total number of bacteria retained on the surface. Statistical significance was ascertained by Student's *t* test.

2.6 Cell culture studies

L929 fibroblast cells were obtained from NCCS, Pune (India) and were maintained in Dulbecco's modified Eagle's medium (DMEM, Gibco Inc. USA) supplemented with 10% v/v fetal bovine serum (FBS, Gibco), 2 mM glutamine (Himedia, India) and the antibiotics namely penicillin and streptomycin (Himedia) at recommended concentrations in a humidified atmosphere of 5% CO_2 at 37°C. As per the requirement for different experiments, confluent flasks were trypsinized and before seeding the cells were counted on a hemocytometer chamber.

2.6.1 *Cell viability and adhesion assays*

The viability of the cell was evaluated under two different conditions namely, on polymer surface and in the presence of medium exposed to them. In the first assay, the polymer samples each of size 1 cm^2 were placed in 24-well plates and exposed to UV light for 15 min. Cells were seeded at a density of approximately 10^4 cells/ml and were incubated at 37°C, in 5% CO_2 atmosphere for 4 h. Following this, the medium was decanted and the polymer films were gently rinsed once with PBS. In the second assay, the cell viability was assessed on glass substrates in the presence of the medium exposed to various polymer surfaces. Glass cover slips of size 1 cm^2 were placed in 24-well plates and exposed to UV light for 15 min. Cells were seeded on different cover slips at a density of approximately 10^4 cells/ml and incubated at 37°C, in 5% CO_2 atmosphere for 24 h to reach confluency. The confluent cells on glass were incubated for 4 h with the polymer films of 1 cm^2 size which were placed by the sides of the wells.

Following both the experiments, the cell viability was determined using a dual staining kit consisting of the membrane-permeant dye Carboxyfluorescein diacetate succinimidyl ester (CFDA SE, Molecular Probes, Invitrogen) and the relatively membrane impermeant nuclear stain propidium iodide (Molecular Probes, Invitrogen) [23–28]. The cells were stained with 5 μM CFDA SE and 500 nM of propidium iodide (PI) in PBS and were incubated at 37°C for 15 min. After incubation the staining solution was decanted and the cells were subjected to further incubation for 30 min at 37°C in PBS containing 100 μg/ml of DNase-free RNase (Fermentas). Cells were then washed with ice cold PBS and fixed with 4% paraformaldehyde. After mounting in Dako cytomation fluorescent mounting media (Dako, USA), the stained cells were examined under a confocal laser scanning microscope (Zeiss LSM 510, Germany) at 60× magnification. Three random fields were selected for each surface to count the live and the dead cells on the cover slips. The percentage of viable cells (without PI staining) per field was determined by multiplying the ratio of viable cells to total cells (live cells plus dead cells) in the field by 100. An average percentage for each polymer was determined from three different fields. A average percentage viability was determined for each sample group from three independent experiments. Statistical comparisons of the mean values between sample groups were made using ANOVA. The number of adherent cells was defined as the number of viable cells in a 60× field. The percentage adhesion was calculated by multiplying the ratio of the % of viable cells on treated substrate to the % of viable cells on glass substrate by 100.

2.7 Real-time PCR (RT-PCR) analysis of TNF-α gene expression

The cytokine TNF-α is one of the most important signaling molecules involved in conducting the response to foreign materials, and its upregulation is considered to be a accurate measure of inflammation [29]. The cytokine TNF-α on different surfaces were quantified at various time points using real-time reverse transcription polymerase chain reaction (RT-PCR) [30]. The UV sterilized polymer films of size 1 cm^2 were placed in a 24-well plate and were incubated with L929 fibroblasts with a cell density of 10^4 cells/ml for 0.5, 1, 1.5, 2 and 4 h. Lipopolysaccharide (LPS) which was a known inducer of TNF-α gene expression was used as positive control along with glass as negative control.

2.7.1 Total RNA extraction

The RNA of the samples taken from each time point was extracted from the cells with TRIzol®-reagent (Invitrogen, USA), as per the instructions of the manufacturer under RNase free conditions. The aqueous portion was extracted with chloroform and the subsequent RNA was precipitated with 70% ethanol in diethylpyrocarbonate treated water and then was purified with RNeasy column (Cat No. 74204, Qiagen). The concentrations of RNA were determined by UV spectrometry using Nanodrop ND-1000 (Thermo Scientific, USA). The quality of RNA was checked by means of denaturing formaldehyde agarose electrophoresis [31].

2.7.2 Deoxyribonuclease I (DNase I) treatment and reverse transcription (RT)

Prior to reverse transcription, all RNA samples were subjected to DNase I (Amersham Pharmacia) treatment at 37°C for 30 min, to remove genomic DNA contamination thereby preventing its carryover to the RT reaction. The samples were then mixed with 70% ethanol and further purified using RNeasy columns (Qiagen). The purified RNA was reverse transcribed using High Capacity cDNA Archive Kit (Applied Biosystems) according to the manufacturer's instructions [31].

2.7.3 Primer design

The mouse gene sequences were downloaded from NCBI database and the primers were designed using the IDT's SciTools Primer Quest [32]. Computational studies using the "blastn" software http://www.ncbi.nlm.nih.gov/BLAST/) revealed that the designed primers were unique for TNF-α and GAPDH (Glyceraldehyde 3 phosphate dehydrogenase). The primer sequences were as follows and for the assay were obtained from MWG Biotech (Bengaluru, India).

AK-TNF-α-F-5′-AGCCGATGGGTTGTACCTTGT CTA-3′;
AK-TNF-α-R-5′-TGAGATAGCAAATCGGCTGAC GGT-3′;
AK-GAPDH-F-5′-TGCACCACCAACTGCTTA-3′;
AK-GAPDH-R-5′-GGATGCAGGGATGATGTT-3′.

2.7.4 Real-time PCR

Real-time PCR was performed using SYBR® Green PCR Master Mix using Applied Biosystem 7300 Real-Time PCR System. The PCR solution contained 2.5 μl of primer mix (final concentration, 166 nM), 7.5 μl of 2× SYBR PCR mix (Applied Biosystems, Foster City, CA), and 5 μl of the sample. Universal thermal PCR cycling conditions suggested by Applied Biosystems were followed and all the samples were normalized to GAPDH.

3 Results

3.1 ATR-FT-IR analysis

The ATR-FT-IR spectra of PU, PU-Curdlan and PU-BSA films are shown in Fig. 1. Spectra of the PU-Curdlan films are notably different from the PU films in the region between 1,060–1,160 cm^{-1} and between 3,300–3,400 cm^{-1} regions. The peak at 1,160 cm^{-1} is assigned to the anti-symmetric stretching of the C_1–O–C_3 bridge of the β-1,3-glucan linkage in curdlan, and the signals at 1,060 cm^{-1} represent the typical C–O bonds. The distinctive absorption bonds at 3,330 cm^{-1} is assigned to –OH vibrations [33]. PU-BSA showed the characteristic IR peaks of amide I and amide II at 1,650 and 1,540 cm^{-1} which could be assigned to –C=O stretching and N–H deformation, respectively. Thus, ATR-FTIR studies indicated that both the molecules were successfully immobilized on the PU surface.

3.2 Dynamic contact angle measurements, surface free energy and in vitro stability of surface films

Virgin PU exhibited typical hydrophobic surface, which was characterized by relatively high values of advancing ($\theta_A = 91.1^\circ$) and receding contact angles ($\theta_R = 84.0^\circ$). The solvent treatment marginally reduced the hydrophobicity. Immobilization of both curdlan and BSA were effective in rendering the surfaces more hydrophilic, which was seen by a reduction in the values of both θ_A and θ_R

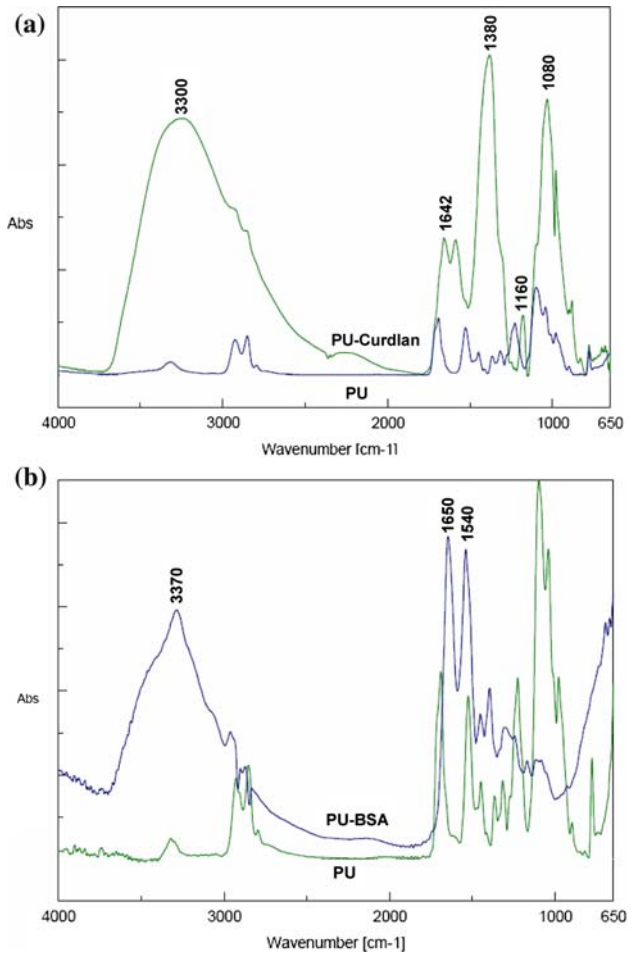

Fig. 1 ATR-FTIR spectra of PU films modified with **a** Curdlan, **b** BSA

Table 1 Dynamic contact angle analysis of modified TecoflexTM film

Polymer	Advancing contact angle (θ_A)	Receding contact angle (θ_R)	Hysteresis ($\theta_A - \theta_R$)
PU	91.1° ± 2.2	84.0° ± 1.3	7.1°
PU-THF	86.8° ± 2.0	78.2° ± 1.8	8.6°
PU-BSA	60.7° ± 3.4	33.1° ± 2.9	27.6°
PU-Curdlan	36.4° ± 4.0	0°	36.4°

Data reported were averaged over 5 measurements

(Table 1). PU-Curdlan showed highest hysteresis, followed by PU-BSA and the least was shown by PU.

The stability of Curdlan and BSA entrapped PU films were determined by contact angle measurements of samples removed from saline solution at different times over a period of 30 days (Table 2). No significant change in the contact angles of both the PU-Curdlan and PU-BSA were noted over this period. However the contact angles increased to pre-coating levels after 12 h for physically adsorbed curdlan and after 2 days for physically adsorbed BSA samples respectively. The total surface free energies and their dispersive and polar components of the surfaces were calculated according to the Fowkes's method and are presented in Table 3. After immobilization, the polar (γ^P) component of the surface free energy significantly increased. The surface free energy of the modified samples showed an increase when compared to the PU, with PU-Curdlan surface showing highest increase followed by PU-BSA.

3.3 SEM-EDAX analysis

SEM-EDAX analysis of the films provided insight into the surface topography and micro-space composition (Fig. 2). Curdlan modification increased the surface roughness while BSA modification led to a relatively smooth surface when compared to unmodified PU. Table 4 shows the elemental composition and the O/C and N/C ratios of these films as calculated from EDAX measurements. Upon curdlan modification the weight percentage of oxygen increased (34.4 ± 1.0%) while carbon did not change significantly. BSA modification increased the weight percent of both carbon (39.3 ± 0.9%) and nitrogen (39.2 ± 1.3%). Thus, SEM-EDAX results also indicated that biomacromolecules have been successfully immobilized onto TecoflexTM surfaces.

3.4 Atomic force microscopy analysis

AFM studies were aimed at visualization of the nanostructure on the polymer surface before and after modification (Fig. 3). The average, maximum and mean roughness of these films are listed in Table 5. PU surface was marginally rough (average roughness of 25 nm) at the atomic level with several islands of about 1,000 nm width (Fig. 3a). Curdlan immobilization increased the surface roughness dramatically (104 nm), and the surface showed large globular structures in several regions (Fig. 3b). However, on treatment with BSA, the polymer surface became highly planar with a few pin holes (Fig. 3c) and the average roughness reduced to 1 nm.

3.5 Confocal laser scanning microscopy (CLSM) investigation

The cross-sectional part of the rhodamine-labeled dextran modified TecoflexTM film is shown in Fig. 4a and b. The figures reveal that both sides of the film were covered with dextran. The thickness of the dextran layer was determined from (Fig. 4b) to be approximately 20–30 μm. Further investigations indicated a change in the

Table 2 Water contact angles for physically adsorbed and entrapped biomacromolecules on Tecoflex surfaces as a function of exposure times to saline solution at 37°C

Days	Contact angle (θ)				
	PU	Physically adsorbed BSA	PU-BSA	PU-CUR	Physically adsorbed Curdlan
Control	86.6 ± 1.7	67.5 ± 7.1	60.7 ± 3.9	34.2 ± 4.3	64.4 ± 8.6
12 h		71.3 ± 5.6	64.3 ± 3.2	36.3 ± 3.6	80.7 ± 3.1
5 days	86.7 ± 1.4	82.1 ± 3.2	67.2 ± 2.2	38.5 ± 3.3	84.3 ± 1.5
10 days	86.4 ± 2.1	84.6 ± 3.4	67.8 ± 2.4	38.9 ± 2.7	84.5 ± 1.2
20 days	86.2 ± 2.5	84.9 ± 3.7	66.9 ± 3.0	40.2 ± 3.4	84.2 ± 1.5
30 days	86.3 ± 1.8	84.5 ± 3.3	67.7 ± 2.8	39.9 ± 3.0	84.6 ± 1.6

Data reported were averaged over 3 measurements

Table 3 Surface free energy and their components of various TecoflexTM surfaces

Sample	Dispersion component (γ^d) (mN/m)	Polar component (γ^p) (mN/m)	Surface energy (γ) (mN/m)
PU	23.6	8.83	32.43
PU-Curdlan	17.9	28.19	46.09
PU-BSA	21.8	19.8	40.98

fluorescence intensity of the entrapped dextran layer from the outside to the inside (Fig. 4c). The fluorescence intensity increased steeply followed by a short stable intensity which may be due to a thin coating layer of the dextran. The fluorescence intensity then decreased gradually, which reveals a decreasing density gradient of the rhodamine-labeled dextran. Thus, the CLSM investigation of the entrapment structure revealed the existence of the entrapment layer about 20–25 μm in depth, confirming the surface entrapment of biomacromolecules on TecoflexTM surface.

3.6 Protein adsorption

The adsorption of bovine fibrinogen (BFG) onto various surfaces from the protein solution (0.1 mg/ml) is shown in Table 6. These results demonstrate that both PU-Curdlan and PU-BSA surfaces are able to decrease fibrinogen adsorption and the later in particular is more effective than the former in reducing fibrinogen adsorption (Fig. 5).

3.7 Short-term bacterial adhesion assays

PU-Curdlan surface significantly reduced *staphylococcus aureus* adhesion when compared to PU and PU-THF control (Fig. 6, $P < 0.05$) in 4 h, while there was no significant change in the adhesion of *pseudomonas aeruginosa.* While it is seen that PU-BSA had lower adhesion of both the species when compared to untreated PU and PU-THF control (Fig. 6, $P < 0.05$).

3.8 Cell viability and adhesion assays

The viability of the cells was monitored on the basis of the appearance of fluorescent nuclei (red) due to the uptake of PI, which indicated dead cells. Cell viability drastically decreased on the surfaces of PU (12.6 ± 0.2%) and PU-THF (12.8 ± 0.3%) when compared to untreated glass which was taken as 100% (Fig. 7, $*P < 0.05$). The viability of cells exposed to PU-Curdlan (98.3 ± 0.6%) and PU-BSA (99.5 ± 0.8%) were comparable to untreated glass control (Fig. 7, $*P < 0.05$). A significant decrease in the percentage cell adhesion was observed on PU-Curdlan (39.0 ± 4.0%) and PU-BSA (34.02 ± 3.6%) surfaces when compared to untreated glass control which was assumed to allow 100% cell adhesion (Fig. 8, $*P < 0.05$).

Cell viability was also evaluated on glass substrates in the presence of the medium exposed to various PU surfaces (Fig. 9). The viability of cells in the presence of the medium exposed to PU significantly decreased on glass when compared to untreated glass which was taken as 100%. While, the cell viability in the presence of the medium exposed to PU-Curdlan and PU-BSA was not affected on glass.

3.9 Real time PCR (RT-PCR) analysis of TNF-α gene expression

The surface induced cellular inflammatory response to various polymers were evaluated by quantifying the expression levels of the proinflammatory cytokine TNF-α

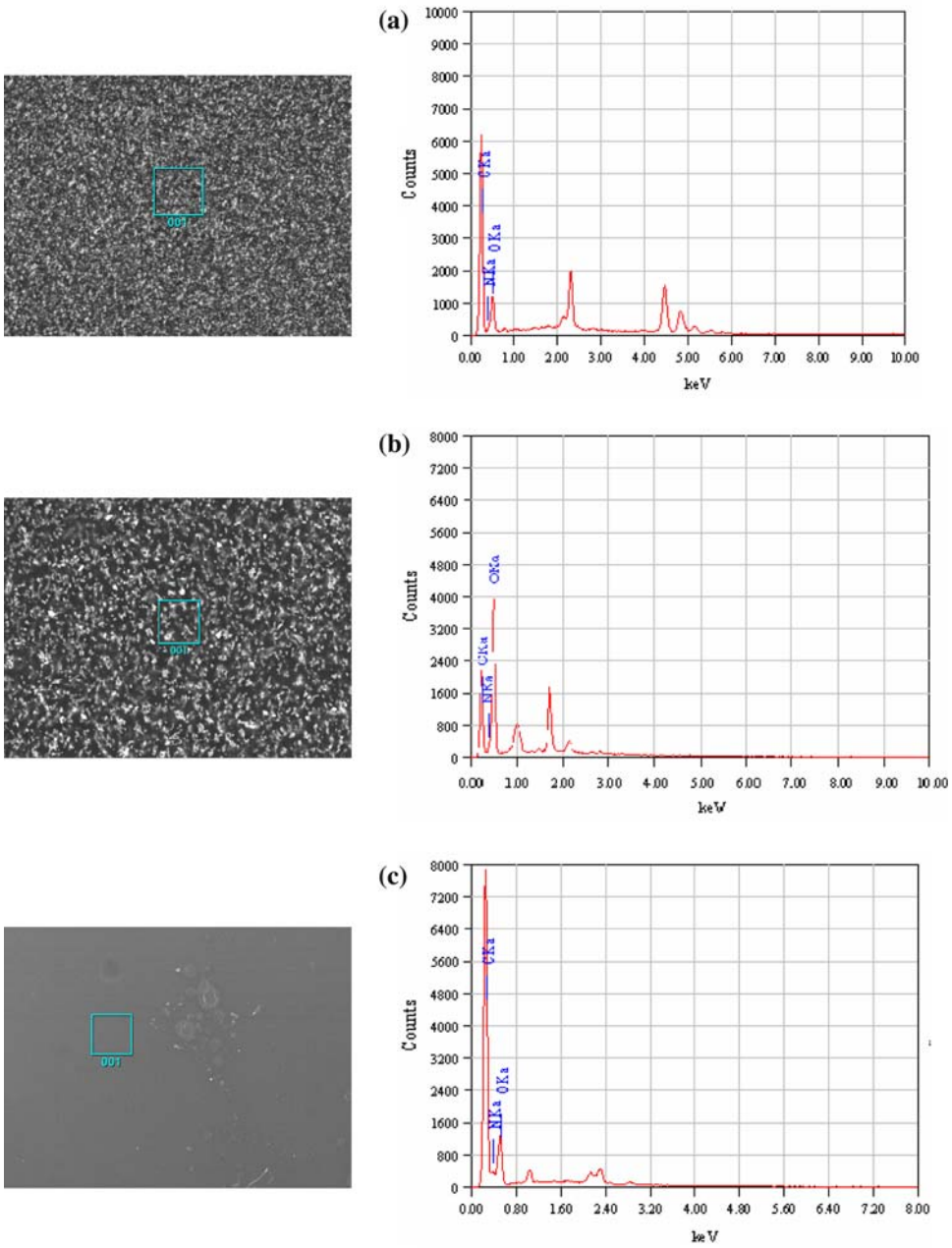

Fig. 2 SEM-EDAX analysis of **a** PU, **b** PU-Curdlan and **c** PU-BSA surfaces

Table 4 Surface elemental composition of modified TecoflexTM films as measured by EDAX

Sample	Wt%				
	C	N	O	O/C	N/C
PU	29.88	27.71	15.54	0.520	0.927
PU-Curdlan	28.85	–	34.45	1.194	–
PU-BSA	39.37	39.22	18.59	0.49	0.996

as a function of time (Fig. 10). The exposure of L929 fibroblasts to LPS stimulated TNF-α transcript levels within 1 h, and the levels increased to a maximum of 1.8 fold to its original value ($^{**}P < 0.001$) in 4 h. TNF-α transcripts peaked within 2 h of exposure to PU and the levels increased further to 1.6 fold to its original value ($^{**}P < 0.001$) in 4 h, which was highest recorded amongst all the samples. Whereas, cells exposed to PU-Curdlan and PU-BSA had only 1.2 ($^{**}P < 0.001$) and 1.1 fold

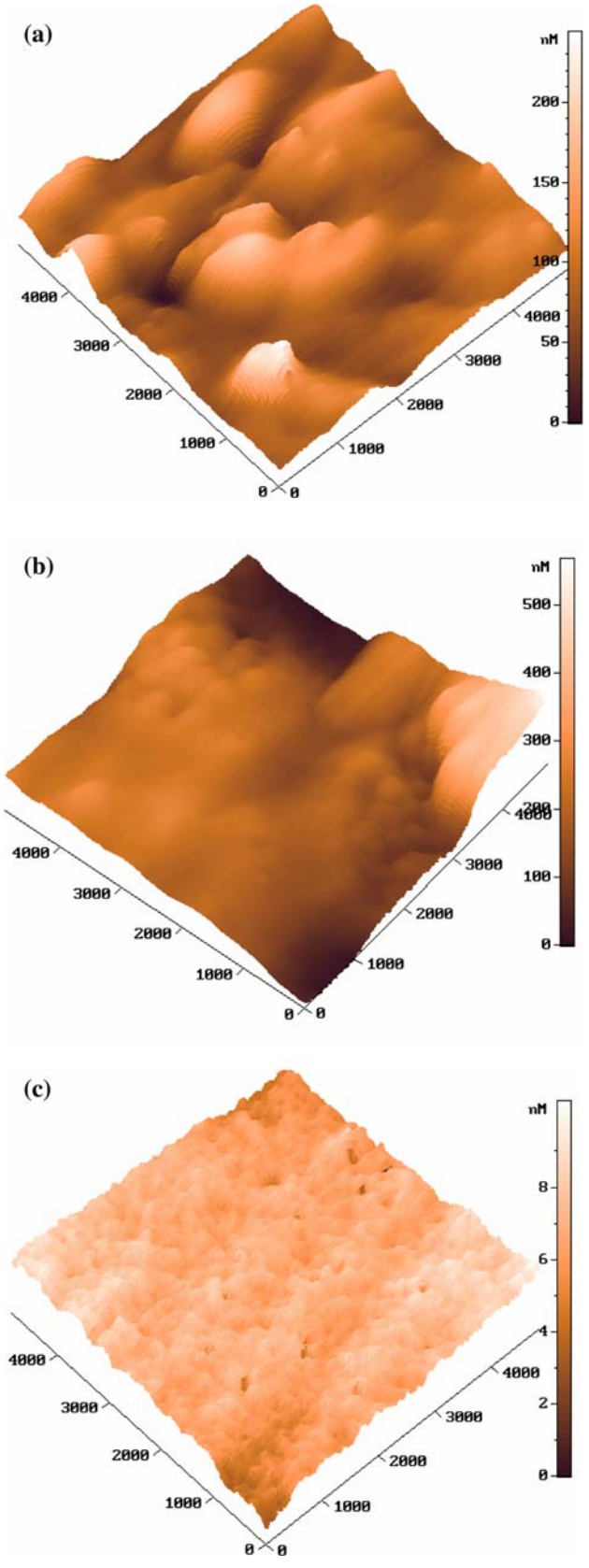

Fig. 3 Typical AFM topographic images of **a** PU, **b** PU-Curdlan and **c** PU-BSA surfaces

Table 5 Roughness of the modified TecoflexTM films

Samples	Average roughness (nm)	Maximum roughness (nm)	Mean roughness (nm)
PU	25	244	93
PU-Curdlan	104	674	346
PU-BSA	1	10	7

($^{**}P < 0.001$) increase in the transcript levels from its original value.

4 Discussion

Immobilization of hydrophilic macromolecular layers on surfaces and its effect upon the extent of non-specific protein and cell adhesion are of considerable interest [34]. This is particularly so in the context of understanding the characteristics of a polymeric biomaterial [35, 36]. The effect of polysaccharides and proteins including dextrans, albumin, laminins on bacterial and cellular interactions with polymers have been studied [37–40]. In those studies the biomolecules were physically adsorbed onto the surfaces. In the present study curdlan was used to modify the surface of TecoflexTM by the entrapment method and its effect on various cell and polymer interactions was evaluated. The entrapment structure created by this solution technique led to high concentration of the modifier near the polymer surface. The entrapment remained intact and stable. Experiments showed low cell adherence and protein adsorption even after 20 days, and also there was no detectable desorption of curdlan in saline even after 30 days.

Protein adsorption is important in the initial conditioning of the material when it is just implanted into the body, and is instrumental in the activation of various inflammatory cascades. It also provides adhesion sites for some bacteria. Serum proteins, such as fibrinogen, fibronectin and vitronectin, play a critical role in cell adhesion on an artificial material [41–44]. It is clear that these plasma proteins have multifacet influence on the biocompatibility of different substrates. Both PU-Curdlan and PU-BSA surfaces reduced protein adsorption when compared to the base, although the later modification was found to be more effective than the former. It is likely that the most effective biocompatible surface will be the surface on which associated proteins are retained in their native conformation. The PU-Curdlan surface may achieve this through their ability to generate a highly hydrated surface that mimics the natural environment encountered by plasma proteins because of its tendency to strongly bind water molecules

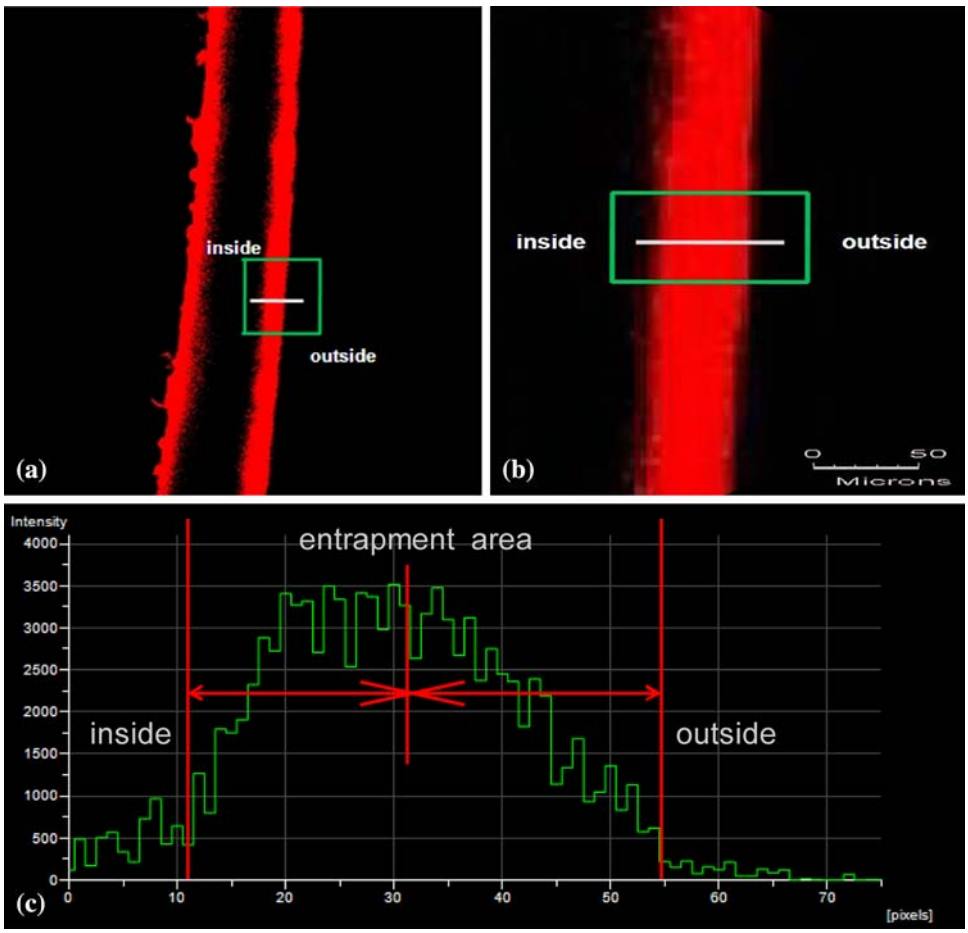

Fig. 4 Confocal laser scanning microscopy investigation of cross-section part of the entrapment film. **a**, **b** Cross-sections of a rhodamine-labeled dextran-modified PU film. **c** Fluorescence intensity of the entrapped dextran layer from outside to inside

Table 6 Adsorption of bovine fibrinogen (BFG) onto surfaces of modified TecoflexTM films

Polymer	BFG adsorption (μg/cm^2)
PU	2.674 ± 0.051
PU-Curdlan	1.983 ± 0.077
PU-BSA	1.650 ± 0.089

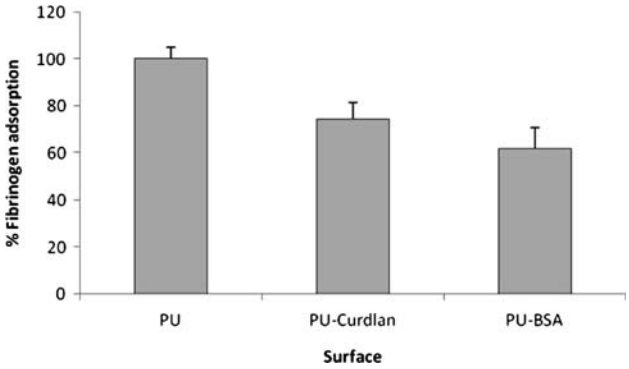

Fig. 5 Adsorption of bovine fibrinogen (BFG) onto the surface of modified TecoflexTM films

leading perhaps to a thermodynamic hydration barrier. The dynamic contact angle and the surface free energy data of PU-Curdlan appear to support this hypothesis. Its surface has lower advancing and receding contact angles (higher surface free energy) when compared to virgin PU or PU-BSA suggesting a greater hydrophilicity and perhaps increased bound water.

Bacterial adhesion is a very complicated process that depends on many surface factors, including chemistry, charge, hydrophobicity, and the presence of protein [45–47]. Although the initial stage of nonspecific attachment of bacteria on a surface is a key determinant in the subsequent formation of biofilm, the molecular basis of this process is not fully understood. The immobilized curdlan on the PU surface significantly reduced the adhesion of *Staphylococcus aureus*, (by 62%) when compared to untreated PU. Whereas, immobilization of BSA considerably decreased the adhesion of both the strains. This is in agreement with previous studies, which showed the inhibitory effect of albumin on bacterial adhesion [48–51].

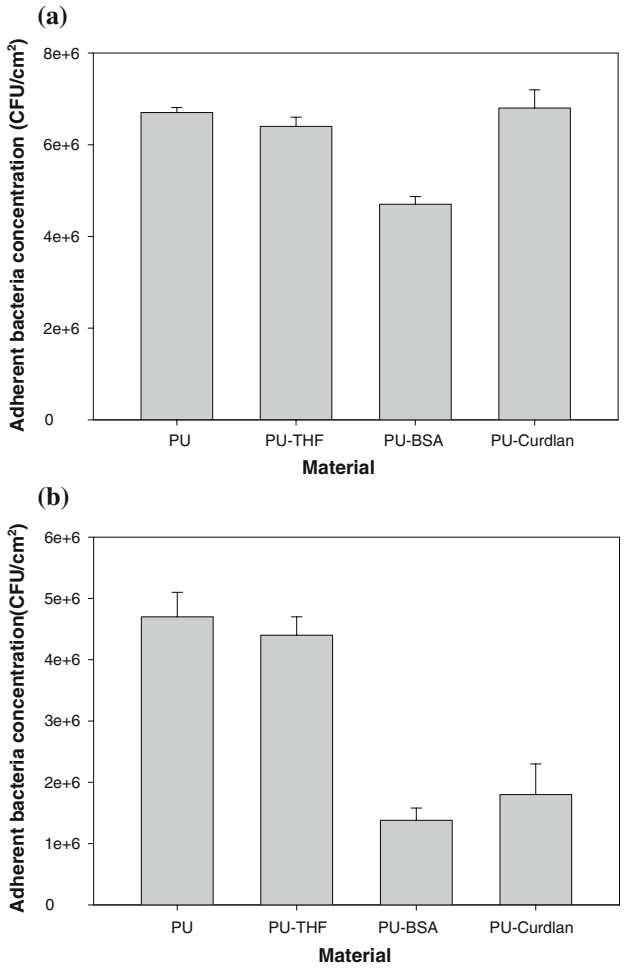

Fig. 6 Bacterial adhesion on materials incubated in approximately 1×10^8 **a** *Pseudomonas aeruginosa* and **b** *Staphylococcus aureus* for 4 h. Mean ± SEM ($n = 3$)

This is attributed to the fact that albumin is an acidic protein with a net negative surface charge, leading to a reduction in the surface hydrophobicity [49, 50]. The reduced adhesion on PU-Curdlan might be a result of steric repulsion between the teichonic acid (also outer membrane proteins) present on gram-positive bacterial surfaces and the hydrophilic curdlan molecules on the PU-Curdlan surfaces. Steric repulsion effects are known to play an important role mainly in adhesion of hydrophobic organisms to hydrophillic surfaces [51, 52]. This result is also supported in literature which reports that increased surface hydrophillicity decreased bacterial adhesion on PU [53, 54]. The resistance of PU-Curdlan and PU-BSA surfaces towards protein adsorption might also be an important factor to note since it is observed that the ability of a surface to resist protein adsorption is a prerequisite to resist bacterial adhesion [55, 56].

The in vitro cell culture studies showed that the base polymer initially induced substantial cytotoxicity on L929 cells, which was successfully suppressed on modified substrates. The number of viable cells significantly decreased on PU and also in the presence of the medium exposed to it, while it was neither affected on the surfaces of PU-Curdlan and PU-BSA nor in the presence of medium exposed to them. Cells adhering to BSA modified substrates showed a rounded morphology for longer incubation periods when compared to curdlan modified substrates. These results are in line with others who have observed reduced protein and cell adhesion on neutral hydrophilic polysaccharide coated substrates [6, 7, 57]. The steric barrier provided by the highly hydrated curdlan molecules minimizes the adsorption of biological fluid-borne proteins and formation of nonselective cell adhesive surface that promotes inflammatory responses. Thus the mechanism of action here must be similar to the complex protein rejection mechanisms observed for other neutral hydrophilic molecules like dextrans and PEG [6, 7, 56–58]. Real-time PCR analysis of the cytokine TNF-α gene expression provided further confirmation that there were quantitative differences in the inflammatory response of L929 fibroblast cells to unmodified and modified surfaces. Virgin PU surface triggered greater stimulation of TNF-α gene expression (highest recorded amongst all the polymeric samples) whereas the levels on PU-Curdlan and PU-BSA showed a modest increase from the base value, indicating that these modifications suppressed the inflammatory response elicited by the base polymer.

BSA is already a known passivating agent in clinical applications, and in the current studies curdlan based substrate was found to be comparable to BSA based substrate. If curdlan coatings are to be utilized for biomaterial implants they should be biocompatible and stable. As found with other neutral hydrophilic polysaccharides like dextrans the surface-bound curdlan on biomaterial surfaces are biocompatible as it mimics the glycocalyx on cell surfaces [1]. Gene expression studies of proinflammatory cytokine TNF-α reveals that the surface bound curdlan does not trigger any inflammatory response in cells. Arakawa et al. [59] assessed curdlan immunogenicity in groups of four CH3 mice, which were given a single intravenous injection of 10 μg curdlan, 10 μg dextran, and 0.1 mg alum-precipitated bovine serum albumin. Although the last two compounds induced a strong passive haemagglutination reaction, curdlan did not induce any reactive antibodies. Therefore it could be assumed that the release of curdlan from the material surface will also not trigger any immune response. Since β-(1 → 3)-glucanases, the enzymes that degrade curdlan, are produced only by some bacteria and fungi and not by human tissues, curdlan coatings on implants will not degrade enzymatically in most tissues. Enzymatic degradation will only occur in tissues that have significant microbial populations,

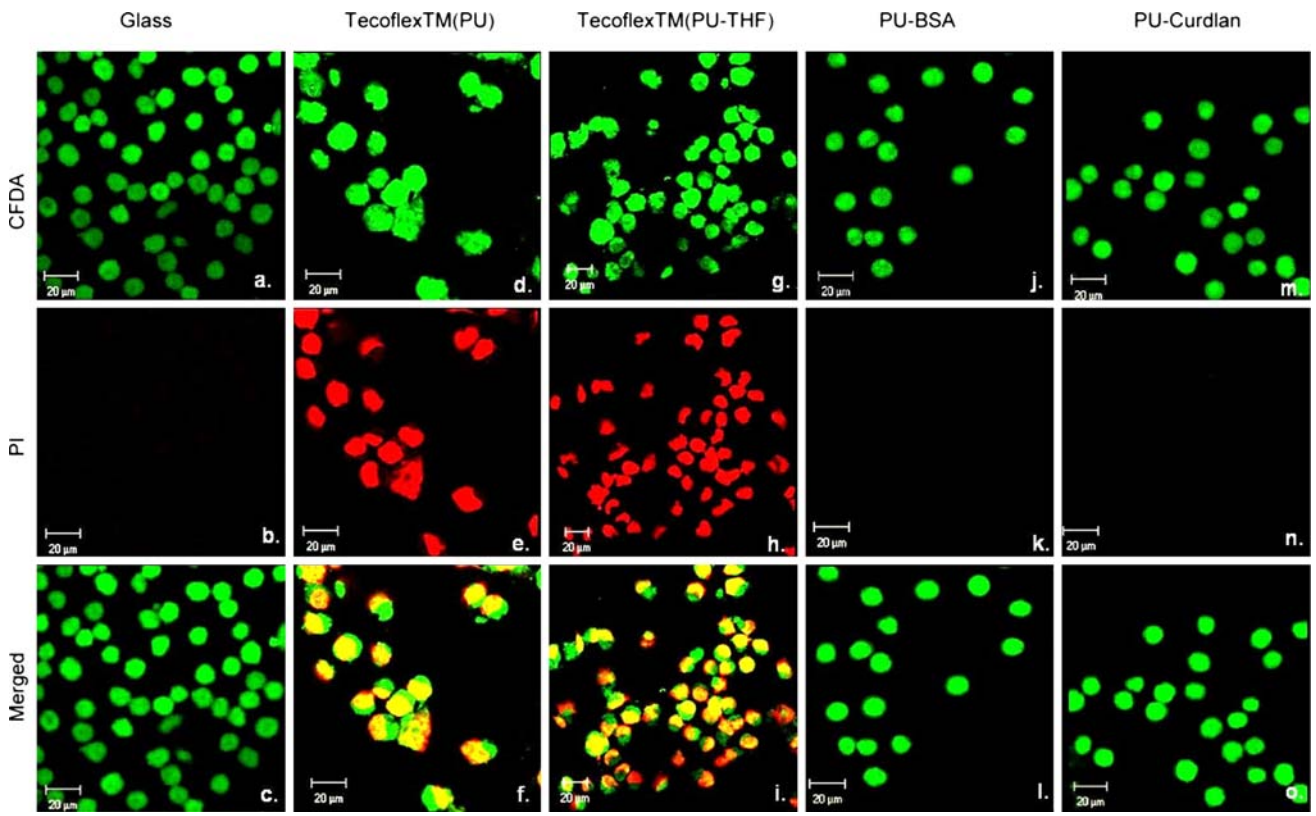

Fig. 7 Confocal laser scanning microscopy of L929 fibroblast cells stained after 4 h for viability on (Panels **a**, **b**, **c**) Control Glass; (Panels **d**, **e**, **f**) cells incubated with PU; (Panels **g**, **h**, **i**) cells incubated with PU-THF; (Panels **j**, **k**, **l**) cells incubated with PU-BSA; (Panels **m**, **n**, **o**) cells incubated with PU-Curdlan

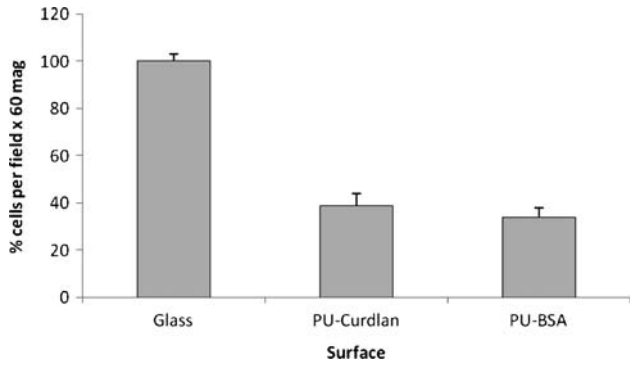

Fig. 8 Adhesion of L-929 mouse fibroblasts to various TecoflexTM surfaces incubated with approximately 1×10^4 cells after 4 h. ($n = 5$)

e.g. gastrointestinal and nasal tracts and hence surface-immobilized curdlan on biomaterials may be quite stable in most of the tissue environments. Also with the multivalent nature of curdlan, further studies should be conducted with curdlan coatings on biomaterials for low protein/cell binding applications and for developing biomimetic cell type selective surface modifications. Since the reported method of curdlan entrapment is inexpensive and a relatively simple process, it may have broad biomedical applications.

5 Conclusions

It is demonstrated by means of ATR-FT-IR, AFM and SEM-EDAX analysis that curdlan and bovine serum albumin can be immobilized on TecoflexTM surface by entrapping them during the reversible swelling of the base polymer. Contact-angle measurements showed that modified films were more hydrophilic than the unmodified polymer. CLSM analysis of the modified surfaces revealed the existence of the entrapment layer about 20–25 µm in depth. The performance of curdlan and BSA modified TecoflexTM surfaces in cell/serum environment demonstrated the success of this entrapment strategy as the modified polymers showed better ability to inhibit protein adsorption, bacterial and cellular interactions at the surface. The expression levels of TNF-α transcript was significantly lower upon exposure to modified films than that to TecoflexTM. These studies have revealed that this

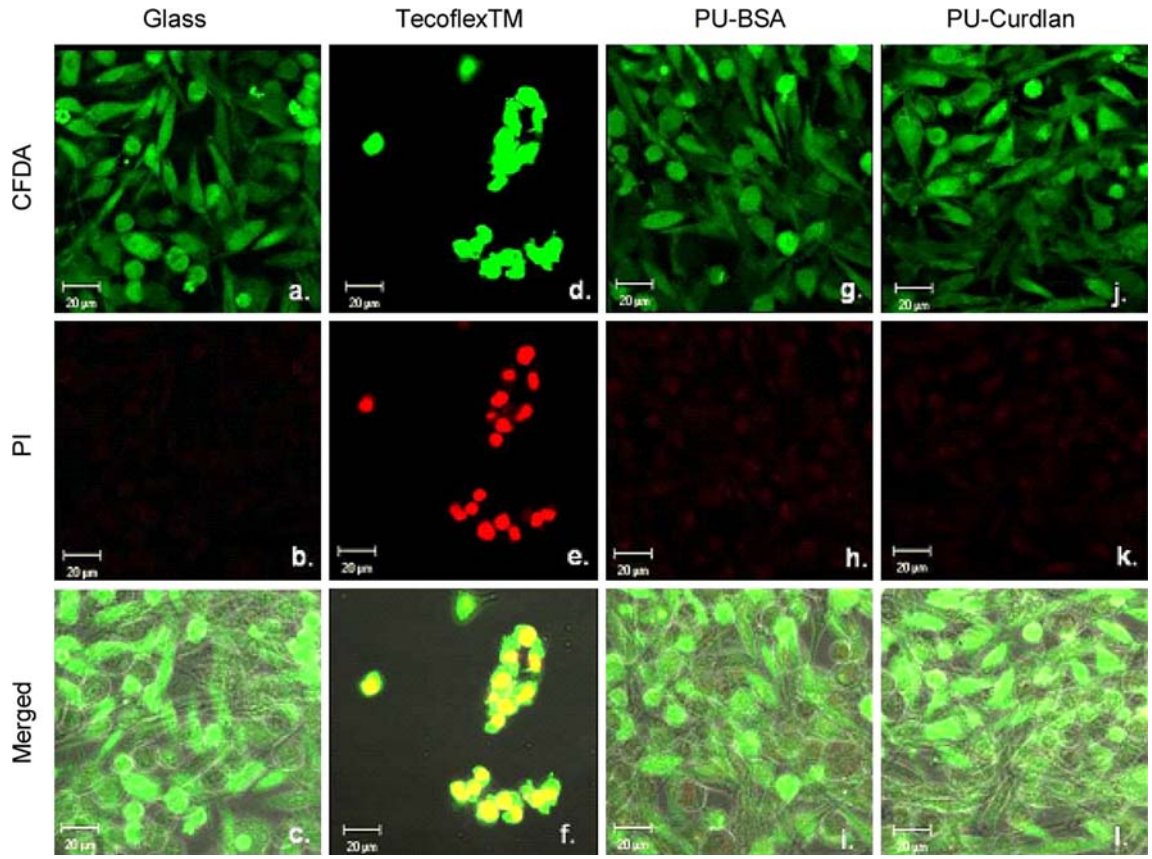

Fig. 9 L929 fibroblast cell viability after 4 h in the presence of medium exposed to (Panels **a**, **b**, **c**) Control Glass; (Panels **d**, **e**, **f**) cells exposed to PU; (Panels **g**, **h**, **i**) cells exposed to PU-BSA; (Panels **j**, **k**, **l**) cells exposed to PU-Curdlan

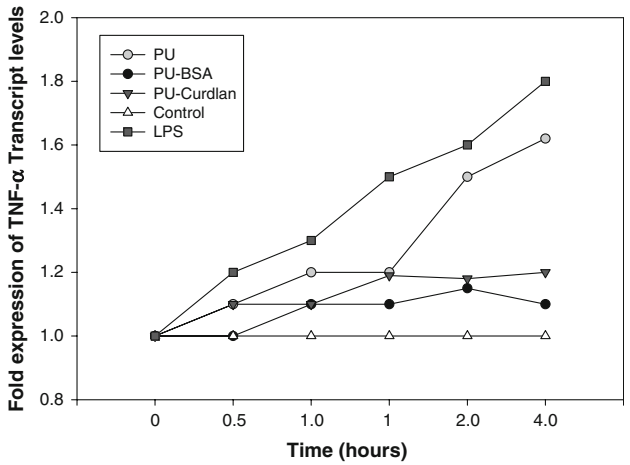

Fig. 10 Effect of various Tecoflex surfaces on expression of TNF-α mRNA in L929 fibroblast cells at different time intervals as determined by Real time PCR analysis. Each time point represents the mean of triplicate measurements ±SD

approach may potentially be used to create materials capable of preventing nonspecific adhesion events, and suppress cytotoxicity, and surface induced cellular inflammatory responses. This simple surface entrapment method would also be useful for applications in the fields of drug delivery, implanted devices and tissue engineering.

Acknowledgements This work was partially funded by DBT. A.K and D.P would like to thank CSIR for providing JRF to pursue their doctoral studies.

References

1. N.B. Holland, Y. Qiu, M. Ruegsegger, R.E. Marchant, Biomimetic engineering of non-adhesive glycocalyx-like surfaces using oligosaccharide surfactant polymers. Nature **392**, 799–801 (1998). doi:10.1038/33894
2. W.H. Evans, J.M. Graham, *Membrane Structure and Function* (Oxford University Press, New York, 1991), pp. 1–86
3. M. Fukuda, Cell surface carbohydrates, in *Molecular Glycobiology*, ed. by M. Fukuda, O. Hindsgaul (Oxford University Press, New York, 1994), pp. 1–52
4. P. Bongrand (ed.), *Physical Basis of Cell–Cell Adhesion* (CRC Press, Boca Raton, 1988), pp. 1–37
5. M.N. Helmus, J.A. Hubbell, Material's selection. Cardiovasc. Pathol. **2**(suppl.), 53S–71S (1993). doi:10.1016/1054-8807(93)90047-6
6. E. Osterberg, K. Bergstrom, K. Holmberg, J.A. Riggs, J.M. Vanalstine, T.P. Schuman et al., Comparison of polysaccharide and poly (ethylene glycol) coatings for reduction of protein

adsorption on polystyrene surfaces. Colloids Surf. A Physicochem. Eng. Aspects **77**, 159–169 (1993)
7. E. Osterberg, K. Bergstrom, K. Holmberg, T.P. Schuman, J.A. Riggs, N.L. Burns et al., Protein-rejecting ability of surface-bound dextran in end-on and side-on configurations: comparison to PEG. J. Biomed. Mater. Res. **29**, 741–747 (1995). doi:10.1002/jbm.820290610
8. N. Ma, M. Tabrizian, A. Petit, O.L. Huk, L.H. Yahia, Cytotoxic reaction and TNF-α response of macrophages to polyurethane particles. J. Biomater. Sci. Polym. Ed. **13**, 257–272 (2002). doi:10.1163/156856202320176510
9. S. Gogolewski, Biomedical polyurethanes, in *Desk Reference of Functional Polymers, Synthesis and Application*, ed. by R. Arshady (American Chemical Society, Washington, DC, 1996), p. 678
10. N.R. James, J. Philip, A. Jayakrishnan, Polyurethanes with radiopaque properties. Biomaterials **27**, 160–166 (2006). doi:10.1016/j.biomaterials.2005.05.099
11. D.W. Renn, Purified curdlan and its hydroxyalkyl derivatives: preparation, properties and applications. Carbohydr. Polym. **33**, 219–225 (1997). doi:10.1016/S0144-8617(97)00058-1
12. B.S. Kim, I.D. Jung, J.S. Kim, J.H. Lee, I.Y. Lee, K. Bok, Curdlan gels as protein drug delivery vehicles. Biotechnol. Lett. **22**, 1127–1130 (2000). doi:10.1023/A:1005636205036
13. T. Yoshida, Y. Tasuda, T. Uryu, H. Nakashima, N. Yamamoto, T. Mimura, Y. Kaneko, Synthesis and in vitro inhibitory effect of -glucosyl-branched curdlan sulfates on AIDS virus infection. Macromolecules **27**, 6272–6276 (1994). doi:10.1021/ma00100a007
14. K. Katsuraya, T. Shoji, K. Inazawa, H. Nakashima, N. Yamamoto, T. Uryu, Synthesis of sulfated alkyl Laminara-oligosaccharides having potent anti-HIV activity and relationship between structure and biological activity. Macromolecules **27**, 6695–6699 (1994). doi:10.1021/ma00101a001
15. A. Greinacher, S. Alban, V. Dummel, G. Franz, C. Mueller-Eckhardt, Characterization of the structural requirements for a carbohydrate based anticoagulant with a reduced risk of inducing the immunological type of heparin-associated thrombocytopenia. Thromb. Haemost. **74**, 886–892 (1995)
16. M.S. Lord, C. Modin, M. Foss, M. Duch, A. Simmons, Monitoring cell adhesion on tantalum and oxidised polystyrene using a quartz crystal microbalance with dissipation. Biomaterials **27**, 4529–4537 (2006). doi:10.1016/j.biomaterials.2006.04.006
17. D.M. Brunette, A. Khakbaznejad, M. Takekawa, M. Shimonishi, H. Murakami, M. Wieland et al., Improving the bio-implant interface by controlling cell behaviour using surface topography, in *Bioimplant Interface. Improving Biomaterials and Tissue Reactions*, ed. by J.E. Ellingsen, S.P. Lyngstadaas (CRC Press, Boca Raton, FL, 2003)
18. N.P. Desai, J.A. Hubbell, Surface physical interpenetrating networks of poly (ethylene terephthalate) and poly(ethylene oxide) with biomedical applications. Macromolecules **25**, 226–232 (1992). doi:10.1021/ma00027a038
19. N.P. Desai, J.A. Hubbell, Solution technique to incorporate polyethylene oxide and other water soluble polymers into surfaces of polymeric biomaterials. Biomaterials **12**, 144–153 (1991). doi:10.1016/0142-9612(91)90193-E
20. R.A. Quirk, M.C. Davies, S.J.B. Tendler, K.M. Shakesheff, Surface engineering of poly (lactic acid) by entrapment of modifying species. Macromolecules **33**, 258–260 (2000). doi:10.1021/ma9916133
21. I.G. Russ, Energy dispersive X-ray analysis, the scanning electron microscope in energy dispersive X-ray analysis, STP 485. (American Society for Testing and Materials, Philadelphia, 1971), p. 154
22. T. Egyhazi, J. Scholtz, V.S. Beskov, SEM-EDAX investigations of use-related microstructural changes in an ammonia synthesis catalyst. React. Kinet. Catal. Lett. **24**, 1–8 (1984). doi:10.1007/BF02069592
23. T. Mosmann, Rapid colorimetric assay for cellular growth and survival: application to proliferation and cytotoxicity assays. J. Immunol. Methods **65**, 55–63 (1983). doi:10.1016/0022-1759(83)90303-4
24. R. Zange, Y. Li, T. Kissel, Biocompatibility testing of ABA copolymers consisting of poly (l-lactic-co-glycolic acid) A blocks attached to a central poly (ethylene oxide) B block under in vitro conditions using different L929 mouse fibroblast cell culture models. J. Control Release **56**, 249–258 (1998). doi:10.1016/S0168-3659(98)00093-5
25. D.L. Garner, D. Pinkel, L.A. Johnson, M.M. Pace, Assessment of spermatozoal function using dual fluorescent staining and flow cytometric analyses. Biol. Reprod. **34**, 127–138 (1986). doi:10.1095/biolreprod34.1.127
26. D.L. Garner, L.A. Johnson, C.H. Allen, Fluorometric evaluation of cryopreserved bovine spermatozoa extended in egg yolk and milk. Theriogenology **30**, 369–378 (1988). doi:10.1016/0093-691X(88)90184-7
27. P.F. Watson, E. Kunze, P. Cramer, R.H. Hammerstedt, A comparison of critical osmolarity and hydraulic conductivity and its activation energy in fowl and bull spermatozoa. J. Androl. **13**, 131–138 (1992)
28. D.L. Garner, L.A. Johnson, Viability assessment of mammalian sperm using SYBR-14 and propidium iodide. Biol. Reprod. **53**, 276–284 (1995). doi:10.1095/biolreprod53.2.276
29. S.B. Goodman, Does the immune system play a role in loosening and osteolysis of total joint replacements? J. Long Term Eff. Med. Implants **6**(2), 91–101 (1996)
30. T. Suzuki, P.J. Higgins, D.R. Crawford, Control selection for RNA quantitation. Biotechniques **29**(2), 332–337 (2000)
31. S.A. Bustin, Absolute quantification of mRNA using real-time reverse transcription polymerase chain reaction assays. J. Mol. Endocrinol. **25**(2), 169–193 (2000). doi:10.1677/jme.0.0250169
32. T.H. Harris, N.M. Cooney, J.M. Mansfield, D.M. Paulnock, Signal transduction, gene transcription, and cytokine production triggered in macrophages by exposure to trypanosome DNA. Infect. Immun. **74**, 4530–4537 (2006). doi:10.1128/IAI.01938-05
33. Y. Jin, H. Zhang, Y. Yin, K. Nishinari, Comparison of curdlan and its carboxymethylated derivative by means of Rheology, DSC, and AFM. Carbohydr. Res. **341**, 90–99 (2006). doi:10.1016/j.carres.2005.11.003
34. J.L. Brash, T.A. Horbett, Proteins at interfaces: an overview, in *Proteins at Interfaces. II. Fundamentals and Applications, ACS Symposium Series*, vol. 602, ed. by T.A. Horbett, J.L. Brash (American Chemical Society, Washington, DC, 1995), pp. 1–23
35. B.D. Ratner, Characterization of biomaterial surfaces. Cardiovasc. Pathol. **2**, 87S–100S (1993). doi:10.1016/1054-8807(93)90049-8
36. J.M. Courtney, N.M.K. Lamba, S. Sundaram, C.D. Forbes, Biomaterials for blood-contacting applications. Biomaterials **15**, 737–744 (1994). doi:10.1016/0142-9612(94)90026-4
37. J.A. Hubbell, Chemical modification of polymer surfaces to improve biocompatibility. Trends Polym. Sci. (Regul. Ed.) **2**, 20–25 (1994)
38. B. Montdargent, D. Letourneur, Toward new biomaterials. Infect. Control Hosp. Epidemiol. **27**, 404–410 (2000)
39. S. Galliani, A. Cremieux, A. VanDerAuwera, M. Viot, Influence of strain, biomaterial, proteins and oncostatic chemotherapy on staphylococcus–epidermidis adhesion to intravascular catheters in vitro. J. Lab. Clin. Med. **127**(1), 71–80 (1996)
40. H. Brydon, G. Keir, E. Thompson, R. Bayston, R. Hayward, W. Harkness, Protein adsorption to hydrocephalus shunt catheters: CSF protein adsorption. J. Neurol. Neurosurg. Psychiatry **64**, 643 (1998)
41. M. Herrmann, P.E. Vaudaux, D. Pittet, R. Auckenthaler, P.D. Lew, F. Schumacherperdreau, G. Peters, F.A. Waldvogel, Fibronectin,

fibrinogen, and laminin act as mediators of adherence of clinical staphylococcal isolates to foreign material. J. Infect. Dis. **158**, 693 (1988)
42. F. Grinnell, M.K. Feld, Fibronectin adsorption on hydrophilic and hydrophobic surfaces detected by antibody binding and analyzed during cell adhesion in serum-containing medium. J. Biol. Chem. **257**, 4888–4893 (1982)
43. T.A. Horbett, M.B. Schway, Correlations between mouse 3T3 cell spreading and serum fibronectin adsorption on glass and hydroxyethylmethacrylate-ethylmethacrylate copolymers. J. Biomed. Mater. Res. **22**, 763–793 (1988). doi:10.1002/jbm.820220903
44. J.G. Steele, G. Johnson, P.A. Underwood, Role of serum vitronectin and fibronectin in adhesion of fibroblasts following seeding onto tissue culture polystyrene. J. Biomed. Mater. Res. **992**(26), 861–864 (2004)
45. Y.H. An, R.J. Friedman, Concise review of mechanisms of bacterial adhesion to biomaterial surfaces. J. Biomed. Mater. Res. **43**, 338–348 (1998). doi:10.1002/(SICI)1097-4636(199823)43:3<338::AID-JBM16>3.0.CO;2-B
46. V.A. Tegoulia, S.L. Cooper, *Staphylococcus aureus* adhesion to self-assembled monolayers: effect of surface chemistry and fibrinogen presence. Colloids Surf. B. Biointerfaces **24**, 217 (2002). doi:10.1016/S0927-7765(01)00240-5
47. D. Pavithra, M. Doble, Biofilm formation, bacterial adhesion and host response on polymeric implants issues and prevention. Biomed. Mater. **3**, 03 4003–03 4017 (2008)
48. H.L. Brydon, R. Bayston, R. Hayward, W. Harkness, Reduced bacterial adhesion to hydrocephalus shunt catheters mediated by cerebrospinal fluid proteins. J. Neurol. Neurosurg. Psychiatry **60**, 671–675 (1996). doi:10.1136/jnnp.60.6.671
49. Y.H. An, R.J. Friedman, R.A. Draughn, E.A. Smith, J.H. Nicholson, J.F. John, Rapid quantification of staphylococci adhered to titanium surfaces using image analyzed epifluorescence microscopy. J. Microbiol. Methods **24**, 29–40 (1995). doi:10.1016/0167-7012(95)00051-8
50. T.J. Kinnari, L.I. Peltonen, T. Kuusela, J. Kivilahti, M. Kononen, J. Jero, Staphylococci and implant surfaces: a review. Otol. Neurotol. **26**, 380 (2005). doi:10.1097/01.mao.0000169767.85549.87
51. H. Tang, A. Wang, X. Liang, T. Cao, S.O. Salley, J.P. McAllister, Adhesion and colonization on silicone. Colloids Surf. B Biointerfaces **51**, 16–24 (2006). doi:10.1016/j.colsurfb.2006.04.011
52. R. Kunz, C. Anders, L. Heinrich, Investigation into the mechanism of bacterial adhesion to hydrogel-coated surfaces. J. Mater. Sci. Mater. Med. **10**, 649–652 (1999). doi:10.1023/A:1008943909728
53. T.D. Brock (ed.), *Biology of Microorganisms* (Prentice-Hall, London, 1997)
54. M.M. Tunney, S.P. Gorman, Evaluation of a poly(vinyl pyrrollidone)-coated biomaterial for urological use. Biomaterials **23**, 4601 (2002). doi:10.1016/S0142-9612(02)00206-5
55. B.D. Ratner, F.J. Hoffmann, J.E. Schoen, F. Lemons, *Biomaterials Science: An Introduction to Materials and Medicine* (Academic Press, New York, 1996)
56. R.G. Chapman, E. Ostuni, M.N. Liang, G. Meluleni, E. Kim, L. Yan et al., Polymeric thin films that resist the adsorption of proteins and the adhesion of bacteria. Langmuir **17**(4), 1225–1233 (2001). doi:10.1021/la001222d
57. S.P. Massia, J. Stark, D.S. Letbetter, Surface-immobilized dextran limits cell adhesion and spreading. Biomaterials **21**, 2253–2261 (2000). doi:10.1016/S0142-9612(00)00151-4
58. R.E. Marchant, S. Yuan, G. Szakalas-Gratzl, Interactions of plasma proteins with a novel polysaccharide surfactant physisorbed to polyethylene. J. Biomater. Sci. Polym. Ed. **6**, 549–664 (1994). doi:10.1163/156856294X00509
59. M. Arakawa, M. Takaoki, H. Kawaji, Immunogenicity of polysaccharide 13140 in rats and mice. Unpublished report from Central Research Laboratories, Takeda Chemical Industries Ltd. Submitted to WHO by Takeda Chemical Industries Ltd. (1974)